International Journal of Control, Automation, and Systems 20(7) (2022) 2260-2272
http://dx.doi.org/10.1007/s12555-021-0401-9
ISSN:1598-6446 eISSN:2005-4092
http://www.springer.com/12555

Enhanced-coupling-based Tracking Control of Double Pendulum Gantry Cranes

Huaitao Shi, Fuxing Yao, Zhe Yuan*, Yunjian Hu, Ke Zhang, and Ling Fu

Abstract: Gantry cranes are mostly regarded as single pendulum models to research. However, gantry cranes will produce a double pendulum effect during the actual operation when the hook mass or cable length between the load and hook cannot be ignored. Aiming at the problems of working inefficiency, poor positioning accuracy and violent hook/load swing during the lifting process of gantry cranes, an enhanced-coupling-based tracking control method is proposed. By referring to a smooth tracking trajectory, the proposed method ensures that the trolley runs steadily. And by combining with the passivity analysis of the gantry crane system, a coupling signal, which enhances the relationship between system variables, is constructed. The system stability is proved strictly by Barbarat theorem and Lyapunov method. Experiments and simulations are performed to demonstrate the feasibility of the proposed method. The final results reflect that the proposed method, which can not only ensure the precise positioning of the trolley, but also restrain and eliminate the system swings promptly, has excellent control performance. When the system parameters are changed or external disturbances are added, the proposed method can also obtain outstanding control performance and has excellent robustness. Not only does the proposed method provide an anti-swing strategy for double pendulum underactuated gantry cranes, but also it provides a possibility for the research and development of the automatic driving of gantry cranes, which has great practical significance and application prospects.

Keywords: Double pendulum, Lyapunov method, nonlinear anti-swing, tracking control, underactuated cranes.

1. INTRODUCTION

Gantry cranes, as a type of large-scale lifting equipment, have the obvious characteristics of flexible application, high reliability and economy. Therefore, they are widely used in various industries such as port logistics, workshop transportation, urban and rural construction [1,2]. As a typical underactuated system, the number of degrees of freedom of gantry crane is more than the number of input variables [3]. Due to the underactuated characteristic, the trolley is prone to produce large system swings during rapid lifting, which affect the precise positioning of the load and the lifting efficiency of the trolley to a certain extent. If not properly controlled, it will even cause serious safety accidents. Therefore, a large number of erudite scholars are devoted to the research of crane anti-swing control, and put forward many anti-swing control strategies, such as sliding mode control [4–6], energy (passive) control [7–9], trajectory planning control [10–12], partial feedback linearization control [13], etc. It is worth considering that in practical engineering, gantry cranes will produce double pendulum swings of the hook and load when there is a cable connection between the hook and load, the length of the cable can not be ignored, and the hook mass can not be much less than the load mass [14]. However, most existing control strategies simplify gantry cranes to single pendulum models for the convenience of dynamic model establishment and anti-swing method design. Therefore, the current researches of single pendulum cranes anti-swing control strategies are mostly difficult to apply to double pendulum cranes. If applied forcedly or operated manually, it will cause low lifting efficiency, poor positioning accuracy, and large hook/load swing, which will cause engineering accidents and affect construction safety. Under this circumstance, relevant domestic and foreign scholars have begun to study the anti-swing strategies of double pendulum cranes successively,

Manuscript received May 13, 2021; revised August 24, 2021; accepted September 21, 2021. Recommended by Associate Editor Ning Sun under the direction of Editor Bin Jiang. This research was supported by the National Science Foundation of China (52075348), in part by the Key Laboratory of Vibration and Control of Aero-Propulsion System, Ministry of Education, Northeastern University (VCAME202001), in part by the Fund Project of Liaoning Provincial Department of Education (lnqn202009), and in part by the Science&Technology Planning Project of MOHURD (2019-K-080).

Huaitao Shi, Fuxing Yao, Zhe Yuan, Yunjian Hu, and Ke Zhang are with the School of Mechanical Engineering, Shenyang Jianzhu University, Shenyang 110168, China (e-mails: sht@sjzu.edu.cn, yfx@stu.sjzu.edu.cn, {yuanzhe, hyj, zhangke}@sjzu.edu.cn). Ling Fu is with the Zoomlion Heavy Industry Science and Technology Co. Ltd., Changsha 410000, China (e-mail: fuling@zoomlion.com).
* Corresponding author.

and have achieved some remarkable results.

At present, the open-loop control strategy based on input shaping is widely applied in double pendulum cranes [15], however, this control strategy has done partial linearizations of the dynamic model and method, which may have large system errors. The partial feedback linearization technology, which reduces the design difficulty of anti-swing controller, is also used in [16] and [17]. Although [15–17] made partial linearizations in the process of designing the anti-swing method, they played a certain role in restraining the hook/load swing, and laid a theoretical foundation for the subsequent anti-swing research. Zhang and Jing proposed a novel adaptive neural network tracking control method [18], which considered several core control problems simultaneously, such as robustness, input dead zone, etc., and achieved excellent control performance. Sun *et al*. proposed an adaptive method [19]. It is worth pointing out that this method does not need exact system model parameters. Chen *et al*. proposed a strategy based on model predictive control for system constraints and input saturation problems [20]. To achieve low energy consumption of the crane system, Wu *et al*. [21] proposed a strategy based on model predictive control. In [22], Sun *et al*. proposed a saturation method, which achieved excellent control effect. However, this method is prone to cause sudden changes in the system swing angles and driving force when the trolley is started. Zhang *et al*. proposed a tracking strategy with reference to a smooth expected trajectory [23]. Not only can this method ensures the stable operation of the trolley, but also it reduces the lifting time and restraints the hook/load swing effectively. However, driven by this method, large residual swing angles still exist when the trolley stops running. Shi *et al*. proposed a control strategy based on energy improvement by enhancing the coupling relationship between system variables [24]. Although this method [24] causes the sudden change of driving force when the trolley is started, it plays an active role in the effective anti-swing and precise positioning of the trolley. Moreover, the robustness analysis by Shi *et al*. [24] is more comprehensive. Interestingly, Zhang and Jing proposed a bioinspired dynamics-based adaptive fuzzy SMC method [25], which considered input dead zone and saturation control. Zhang *et al*. proposed a bioinspired nonlinear dynamics-based adaptive neural network control method [26], which considered uncertain/unknown dynamics and input delay. It is worth pointing out that these advanced control methods [25,26] have guiding significance for the development of crane controller.

An enhanced-coupling-based tracking control method is proposed for gantry cranes. In this method, an undetermined coupling function, which includes the information of the trolley displacement, cable length and swing angles, is constructed by energy analysis, and the function is determined by stability analysis. The proposed method ensures that the trolley starts and runs steadily by referring to a smooth tracking trajectory. Then, the system stability is verified by using Barbalat theorem and Lyapunov method. Ultimately, the performance of the proposed method is analyzed comprehensively, and the effectiveness is proved through a series of simulations and experiments.

The contributions of this paper can be described as follows:

1) In this paper, the double pendulum effect of gantry cranes is considered adequately, and in the process of dynamic model establishment, method design and stability analysis, linearizations or approximations are not applied, which makes the proposed method more accurate in controlling gantry cranes.
2) Not only does the proposed method ensure the smooth operation of the trolley, but also it can restrain and eliminate the system swing angles. The final results reflect that the proposed method has an excellent control effect.
3) Under the condition that the gains remain unchanged, the proposed method has strong robustness to resist the influence caused by the changes of system parameters and external disturbances.

The structure of this paper is stated as follows: The double pendulum gantry crane dynamic model is built in Section 2; an enhanced-coupling-based tracking control method is designed in Section 3, and the system stability is analyzed strictly; the superior control effect and strong robustness of the proposed method are verified through experiments and simulations in Section 4; the conclusion is stated in Section 5.

2. DOUBLE PENDULUM GANTRY CRANE DYNAMIC MODEL

The underactuated gantry crane system is described in Fig. 1, and the system parameters are stated in Table 1. In practice, the mass and elasticity of the cable have negligible impact on the system dynamics [27]; moreover, the

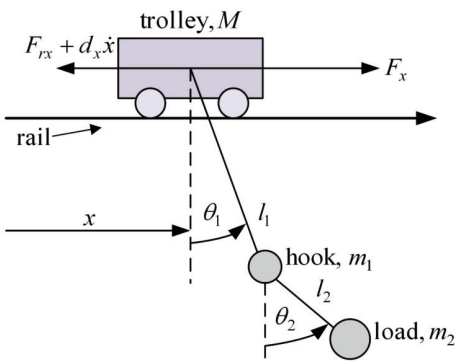

Fig. 1. Double pendulum underactuated gantry crane system.

Table 1. Double pendulum underactuated gantry crane system parameters.

Symbol	Implication	Unit
M	Trolley mass	kg
m_1	Hook mass	kg
m_2	Load mass	kg
x	Trolley displacement	m
l_1	Cable length 1	m
l_2	Cable length 2	m
θ_1	Hook swing angle	deg
θ_2	Load swing angle	deg
F_x	Driving force	N

load does not move to the top of gantry cranes [28–30]. Hence, before establishing double pendulum gantry crane dynamic model, the assumptions are made as follows:

Assumption 1: Ignore the mass and elasticity of the cable.

Assumption 2: The system swing angles should meet:$-\pi/2 < \theta_1, \theta_2 < \pi/2$.

The gantry crane system dynamic model is established by using the Euler-Lagrange equation , and the result is as follows [23,31,32]:

$$\boldsymbol{M}(\boldsymbol{q})\ddot{\boldsymbol{q}}+\mathbf{V}(\boldsymbol{q},\dot{\boldsymbol{q}})\dot{\boldsymbol{q}}+\boldsymbol{G}(\boldsymbol{q})=\boldsymbol{U}+\boldsymbol{F_d}, \tag{1}$$

where $\boldsymbol{q}$ denotes the system state vector, $\boldsymbol{M}(\boldsymbol{q})$ denotes the system inertia matrix, $\boldsymbol{V}(\boldsymbol{q},\dot{\boldsymbol{q}}) \in \mathbb{R}^{3\times3}$ denotes the system centripetal Coriolis force matrix, $\boldsymbol{G}(\boldsymbol{q}) \in \mathbb{R}^3$ denotes the system gravity potential energy vector, $\boldsymbol{U}$ denotes the system control vector, and $\boldsymbol{F_d} \in \mathbb{R}^3$ denotes the system disturbance vector. They are described as follows:

$$\boldsymbol{M}=\begin{bmatrix} M+m_1+m_2 & (m_1+m_2)l_1c_1 & m_2l_2c_2 \\ (m_1+m_2)l_1c_1 & (m_1+m_2){l_1}^2 & m_2l_1l_2c_{1-2} \\ m_2l_2c_2 & m_2l_1l_2c_{1-2} & m_2{l_2}^2 \end{bmatrix},$$

$$\boldsymbol{V}=\begin{bmatrix} 0 & -(m_1+m_2)l_1s_1\dot{\theta}_1 & -m_2l_2s_2\dot{\theta}_2 \\ 0 & 0 & m_2l_1l_2s_{1-2}\dot{\theta}_2 \\ 0 & -m_2l_2l_1\dot{\theta}_1s_{1-2} & 0 \end{bmatrix},$$

$$\boldsymbol{G}=[0 \quad (m_1+m_2)gl_1s_1 \quad m_2gl_2s_2]^T,$$

$$\boldsymbol{U}=[F_x \quad 0 \quad 0]^T,$$

$$\boldsymbol{F_d}=\left[-F_{rx}-d_x\dot{x} \quad -d_{\theta_1}\dot{\theta}_1 \quad -d_{\theta_2}\dot{\theta}_2\right]^T,$$

$$\boldsymbol{q}=[x(t) \quad \theta_1(t) \quad \theta_2(t)]^T,$$

where $s_i=\sin\theta_i$, $c_i=\cos\theta_i$, $s_{i\pm j}=\sin(\theta_i\pm\theta_j)$, $c_{i\pm j}=\cos(\theta_i\pm\theta_j)$, $i,j=1,2\,(i\neq j)$. $d_x \in \mathbb{R}^+$ represents the coefficient of air resistance of the trolley, g stands for the acceleration of gravity, $d_{\theta_1} \in \mathbb{R}^+$ and $d_{\theta_2} \in \mathbb{R}^+$represent the coefficients of air resistance of the hook and load respectively [23,33]. F_{rx}, which represents the friction between the trolley and track, is defined as [31,32,34]:

$$F_{rx}=f_{r0x}\tanh\left(\frac{\dot{x}}{\varepsilon_x}\right)+k_{rx}|\dot{x}|\dot{x}, \tag{2}$$

where f_{r0x}, $\varepsilon_x \in \mathbb{R}$ refer to coefficients related to static friction, $k_{rx} \in \mathbb{R}$ refers to coefficient related to viscous friction.

The underactuated gantry crane system has the properties as follows [35]:

Property 1: Matrix $\boldsymbol{M}(\boldsymbol{q})$ is a positive definite symmetric matrix.

Property 2: Matrix $\boldsymbol{M}(\boldsymbol{q})$ and matrix $\boldsymbol{V}(\boldsymbol{q},\dot{\boldsymbol{q}})$ meet the following anti-symmetric relationship:

$$\mathbf{y}^{\mathrm{T}}\left[\frac{1}{2}\dot{\boldsymbol{M}}(\boldsymbol{q})-\boldsymbol{V}(\boldsymbol{q},\dot{\boldsymbol{q}})\right]\mathbf{y}=0,\ \forall\mathbf{y}\in\mathbb{R}^3. \tag{3}$$

To make the method design and stability analysis easier, the dynamic model is rewritten as follows:

$$\begin{aligned}&(M+m_1+m_2)\ddot{x}+(m_1+m_2)l_1\left(\ddot{\theta}_1c_1-\dot{\theta}_1^2s_1\right)\\&\quad+m_2l_2\left(\ddot{\theta}_2c_2-\dot{\theta}_2^2s_2\right)=F_x-F_{rx}-d_x\dot{x},\end{aligned} \tag{4}$$

$$\begin{aligned}&(m_1+m_2)l_1\left(\ddot{x}c_1+{l_1}^2\ddot{\theta}_1+gs_1\right)\\&\quad+m_2l_1l_2\left(\ddot{\theta}_2c_{1-2}+\dot{\theta}_2^2s_{1-2}\right)=-d_{\theta_1}\dot{\theta}_1,\end{aligned} \tag{5}$$

$$m_2l_2\begin{pmatrix}l_1\ddot{\theta}_1c_{1-2}-l_1\dot{\theta}_1^2s_{1-2}\\+gs_2+l_2\ddot{\theta}_2+\ddot{x}c_2\end{pmatrix}=-d_{\theta_2}\dot{\theta}_2. \tag{6}$$

For the underactuated gantry crane system, its control objectives are as follows [36,37]:

1) The motor drives the trolley from the initial position $x(0)$ to the expected position p_{dx}.
2) The hook/load swing angle $\theta_1(t)/\theta_2(t)$ is suppressed and eliminated.

In other words, they can be stated as follows:

$$\lim_{t\to\infty}[x(t) \quad \theta_1(t) \quad \theta_2(t)]^{\mathrm{T}}=[p_{dx} \quad 0 \quad 0]^{\mathrm{T}}. \tag{7}$$

3. MAIN RESULTS

An undetermined function is constructed to strengthen the relationship between the variables of the system, and a smooth S-shape trajectory, which ensures that the trolley starts and runs steadily,is applied. Then, an enhanced-coupling-based tracking control method is proposed. Finally, the system stability is demonstrated by Barbalat theorem and Lyapunov method. The gantry crane control system is described in Fig. 2.

3.1. Method design

Based on the physical analysis of the system shown in Fig. 1, its energy equation can be obtained

$$E(t)=\frac{1}{2}\dot{\boldsymbol{q}}^{\mathrm{T}}\boldsymbol{M}(\boldsymbol{q})\dot{\boldsymbol{q}}+m_2gl_2(1-c_2)$$

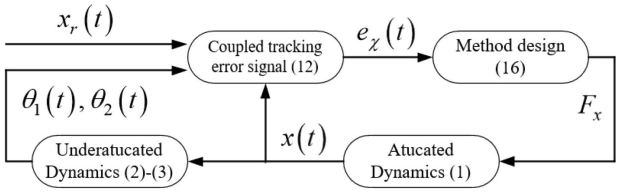

Fig. 2. Double pendulum underactuated gantry crane control system.

$$+(m_1+m_2)gl_1(1-c_1). \tag{8}$$

The first derivative equation of the energy equation shown in (8) is derived. By using the anti-symmetric relation in Property 2 and substituting (4)-(6) into this equation, the following results can be obtained:

$$\begin{aligned}\dot{E}(t) &= \dot{\boldsymbol{q}}^{\mathrm{T}}\left(\boldsymbol{M}(\boldsymbol{q})\ddot{\boldsymbol{q}}+\frac{1}{2}\dot{\boldsymbol{M}}(\boldsymbol{q})\dot{\boldsymbol{q}}\right)\\ &\quad+(m_1+m_2)gl_1\dot{\theta}_1 s_1+m_2gl_2\dot{\theta}_2 s_2\\ &= \dot{x}\left(F_x-F_{rx}-d_x\dot{x}\right)-d_{\theta_1}\dot{\theta}_1^2-d_{\theta_2}\dot{\theta}_2^2.\end{aligned} \tag{9}$$

It can be seen from (9) that the underactuated crane system with F_x as input and $\dot{x}$ as output remains passive. The system has 3 degrees of freedom, but only 1 control quantity. Therefore, to achieve the purpose of restraining the hook/load swing angle, it is of necessity to control the hook/load swing angle in conjunction with the trolley motion. However, if the system swing angles are coupled with the trolley motion rashly, it may lead to poor transient control performance, and even the crane system stability cannot be guaranteed, which may lead to engineering accidents.

To solve this problem, a generalized displacement signal χ, which contains the information of the trolley displacement, the cable length and the system swing angles, is constructed

$$\chi = x+\lambda_1 l_1\int_0^t g(\theta_1)dt+\lambda_2 l_2\int_0^t h(\theta_2)dt, \tag{10}$$

where λ_1, $\lambda_2\in\mathbb{R}^+$ stand for the control gains to be adjusted. $g(\theta_1)$, $h(\theta_2)$ stand for the undetermined functions.

In order to ensure smooth start-up and stable operation of double pendulum underactuated gantry crane system, an S-shaped expected trajectory x_r is quoted here [38]

$$\begin{aligned}x_r(t) &= \frac{p_{dx}}{2}+\frac{{k_v}^2}{4k_a}\ln\left[\cosh\left(\frac{2k_a t}{k_v}-\varepsilon\right)\right]\\ &\quad+\frac{{k_v}^2}{4k_a}\left\{-\ln\left[\cosh\left(\begin{array}{c}\frac{2k_a t}{k_v}-\varepsilon\\ -\frac{2p_{dx}k_a}{{k_v}^2}\end{array}\right)\right]\right\},\end{aligned} \tag{11}$$

where k_v, k_a, ε are the corresponding expected trajectory parameters. The expected trajectory x_r satisfies the following principles [38].

Principle 1: The expected trajectory x_r will gradually converge to the expected position p_{dx}, that is, the expected trajectory x_r is bounded; the first three derivatives $\left(\dot{x}_r(t), \ddot{x}_r(t), {x_r}^{(3)}\right)$ of the expected trajectory x_r, are also bounded and converge to zero. Namely,

$$\begin{aligned}&|x_r(t)|\le p_{dx},\ 0\le\dot{x}_r(t)\le v_{x\max},\\ &|\ddot{x}_r(t)|\le a_{x\max},\ \left|{x_r}^{(3)}(t)\right|\le j_{x\max},\end{aligned}$$

where $v_{x\max}$, $a_{x\max}$ and $j_{x\max}$ stand for the maximum values of the expected trajectory velocity, acceleration and jerk respectively.

A generalized enhanced-coupling-based tracking error signal is constructed by combining (10) with the expected trajectory x_r, as shown below

$$e_\chi = \chi - x_r = x - x_\upsilon, \tag{12}$$

where $x_\upsilon = x_r-\lambda_1 l_1\int_0^t g(\theta_1)dt-\lambda_2 l_2\int_0^t h(\theta_2)dt$.

Then, a coupling tracking error signal vector $\mathbf{e}(t)$ is defined

$$\boldsymbol{e}(t) = \begin{bmatrix}e_\chi & \theta_1 & \theta_2\end{bmatrix}^T. \tag{13}$$

In view of the form of the energy (8), combining (8) and (13), a positive definite scalar equation is constructed for the underactuated gantry crane system

$$\begin{aligned}V(t) &= \frac{1}{2}\dot{\boldsymbol{e}}^{\mathrm{T}}\boldsymbol{M}(\boldsymbol{q})\dot{\boldsymbol{e}}+(m_1+m_2)gl_1(1-c_1)\\ &\quad+m_2gl_2(1-c_2)+\frac{1}{2}k_{px}{e_\chi}^2,\end{aligned} \tag{14}$$

where $k_{px}\in\mathbb{R}^+$ represents the control gain to be adjusted.

Combining (1), (12) and (13), the first derivative equation of (14) with respect to time is obtained by virtue of Property 2

$$\begin{aligned}\dot{V}(t) &= \dot{\boldsymbol{e}}^{\mathrm{T}}\left[\boldsymbol{M}(\boldsymbol{q})\ddot{\boldsymbol{e}}+\frac{1}{2}\dot{\boldsymbol{M}}(\boldsymbol{q})\dot{\boldsymbol{e}}\right]+m_2gl_2\dot{\theta}_2 s_2\\ &\quad+(m_1+m_2)gl_1\dot{\theta}_1 s_1+k_{px}e_\chi\dot{e}_\chi\\ &= \dot{e}_\chi\begin{bmatrix}F_x-F_{rx}-d_x\dot{x}-k_{px}e_\chi\\ -(M+m_1+m_2)\ddot{x}_\upsilon\end{bmatrix}\\ &\quad-\ddot{x}_\upsilon(m_1+m_2)l_1c_1\dot{\theta}_1-\ddot{x}_\upsilon m_2l_2c_2\dot{\theta}_2\\ &\quad-d_{\theta_1}\dot{\theta}_1^2-d_{\theta_2}\dot{\theta}_2^2.\end{aligned} \tag{15}$$

To meet the practical requirements of the gantry crane system, combining the structural form of $\dot{V}(t)$ in (15), the following conditions shall be met: $\dot{e}_\chi\left[F_x-F_{rx}-d_x\dot{x}-(M+m_1+m_2)\ddot{x}_\upsilon-k_{px}e_\chi\right]\le 0$. Therefore, the closed-loop feedback anti-swing method of the underactuated gantry crane system is designed as follows:

$$F_x = F_{rx}+d_x\dot{x}-k_{px}e_\chi-k_{dx}\dot{e}_\chi$$

$$+(M+m_1+m_2)\ddot{x}_\upsilon, \tag{16}$$

where $k_{dx} \in \mathbb{R}^+$ represents the control gain to be adjusted, and the determination of function $g(\theta_1)$ and function $h(\theta_2)$ in x_υ will be given in combination with stability analysis.

Remark 1: In the actual control of the gantry crane system, the state constraint problem is very important to ensure the safety of the system. The proposed method refers to a smooth S-shaped expected trajectory x_r. However, although the expected trajectory x_r can be constrained by setting its maximum velocity and maximum acceleration, the trolley displacement and load position are difficult to be constrained. Fortunately, Chen and Sun successfully solved both actuated and unactuated state constraints for a class of underactuated systems in [39]. When controlling the crane system actually in the future, the proposed method can constrain the system states by the following methods: 1) Combined with the actuated state constraint function $\Delta_1(t)$ in [39], the proposed method can consider quoting function $\Delta_1(t) = \frac{\alpha}{2}\frac{{e_x}^2}{(e_x-\zeta_M)^2(e_x+\zeta_m)^2}$ to constraint the trolley displacement x, where $\alpha \in \mathbb{R}^+$ represents the positive control gain, e_x is the simple expression of $x-x_r$, ζ_m and ζ_M represent the lower and upper bounds of e_x, respectively; 2) combined with the unactuated state constraint function $\Delta_2(t)$ in [39], the proposed method can constrain the unactuated states θ_1 and θ_2; 3) combined with the composite variable constraint function $\Delta_3(t)$ in [39], the proposed method can constrain the load position. For the design and analysis of specific actuated and unactuated state constraint functions, please refer to [39].

3.2. Stability analysis

Theorem 1: The enhanced-coupling-based tracking control method (16) can ensure that the trolley arrives the expected position precisely, while restraining and eliminating the system swing angles effectively, namely

$$\lim_{t\to\infty}\begin{bmatrix} x(t) & \dot{x}(t) & \theta_1(t) & \dot{\theta}_1(t) & \theta_2(t) & \dot{\theta}_2(t)\end{bmatrix}^T = \begin{bmatrix} p_{dx} & 0 & 0 & 0 & 0 & 0\end{bmatrix}^T.$$

Proof: The positive scalar function $V(t)$ in (14) is chosen as the Lyapunov candidate function, its first derivative equation with respect to time is derived, and the enhanced-coupling-based tracking control method (16) with x_υ is substituted into the equation. After sorting out, the following equation can be obtained

$$\begin{aligned}\dot{V}(t) = {} & \lambda_1(m_1+m_2)\left[c_1\dot{\theta}_1 + \frac{m_2 l_2}{(m_1+m_2)l_1}c_2\dot{\theta}_2\right] \\ & \times\left(g'(\theta_1)\dot{\theta}_1 + \frac{\lambda_2 l_2}{\lambda_1 l_1}h'(\theta_2)\dot{\theta}_2\right){l_1}^2 \\ & -\left[(m_1+m_2)l_1c_1\dot{\theta}_1 + m_2 l_2 c_2\dot{\theta}_2\right]\ddot{x}_r \\ & -k_{dx}\dot{e}_\chi^2 - d_{\theta_1}\dot{\theta}_1^2 - d_{\theta_2}\dot{\theta}_2^2.\end{aligned} \tag{17}$$

It is known that the cable length between the trolley and hook satisfies $l_1(t) > 0$, then combining with (17), and finally using the properties of arithmetic geometric mean inequality, the following conclusions can be deduced

$$\begin{aligned} & -\left[(m_1+m_2)l_1c_1\dot{\theta}_1 + m_2 l_2 c_2\dot{\theta}_2\right]\ddot{x}_r \\ & \le (m_1+m_2)l_1\left[c_1\dot{\theta}_1 + \frac{m_2 l_2}{(m_1+m_2)l_1}c_2\dot{\theta}_2\right]^2 \\ & \quad + \frac{1}{4}(m_1+m_2)l_1\ddot{x}_r^2.\end{aligned} \tag{18}$$

Combining (17), (18) can be expanded and contracted. After sorting out, the result is as follows:

$$\begin{aligned}\dot{V}(t) \le {} & \lambda_1{l_1}^2\left(g'(\theta_1)\dot{\theta}_1 + \frac{\lambda_2 l_2}{\lambda_1 l_1}h'(\theta_2)\dot{\theta}_2\right) \\ & \times(m_1+m_2)\left[c_1\dot{\theta}_1 + \frac{m_2 l_2}{(m_1+m_2)l_1}c_2\dot{\theta}_2\right] \\ & +(m_1+m_2)l_1\left[c_1\dot{\theta}_1 + \frac{m_2 l_2}{(m_1+m_2)l_1}c_2\dot{\theta}_2\right]^2 \\ & -d_{\theta_1}\dot{\theta}_1^2 - d_{\theta_2}\dot{\theta}_2^2 - k_{dx}\dot{e}_\chi^2 \\ & +\frac{1}{4}(m_1+m_2)l_1\ddot{x}_r^2.\end{aligned} \tag{19}$$

Taking into account the actual operating conditions of gantry cranes, the term, which containing the system swing Angle $\dot{\theta}_1$, $\dot{\theta}_2$ in $\dot{V}(t)$, shall be non-positive value, and then the relation can be determined as follows:

$$\begin{cases} g'(\theta_1) = -\cos\theta_1, \\ h'(\theta_2) = -\cos\theta_2, \end{cases} \Rightarrow \lambda_2 = \frac{m_2}{(m_1+m_2)}\lambda_1. \tag{20}$$

By substituting (20) into (19), it can be seen that

$$\begin{aligned}\dot{V}(t) \le {} & (m_1+m_2)\left[c_1\dot{\theta}_1 + \frac{m_2 l_2}{(m_1+m_2)l_1}c_2\dot{\theta}_2\right]^2 \\ & \times(1-\lambda_1 l_1)l_1 + \frac{1}{4}(m_1+m_2)l_1\ddot{x}_r^2 \\ & -k_{dx}\dot{e}_\chi^2 - d_{\theta_1}\dot{\theta}_1^2 - d_{\theta_2}\dot{\theta}_2^2 \\ \le {} & -k_{dx}\dot{e}_\chi^2 + \frac{1}{4}(m_1+m_2)l_1\ddot{x}_r^2 \\ & -d_{\theta_1}\dot{\theta}_1^2 - d_{\theta_2}\dot{\theta}_2^2,\end{aligned} \tag{21}$$

where $\lambda_1 l_1 > 1$.
By deducing the first-order integral of both sides of (21), it can be deduced as follows:

$$\begin{aligned}V(t) \le {} & V(0) - k_{dx}\int_0^t \dot{e}_\chi^2 d\tau \\ & -d_{\theta_1}\int_0^t \dot{\theta}_1^2 d\tau - d_{\theta_2}\int_0^t \dot{\theta}_2^2 d\tau \\ & +\frac{1}{4}(m_1+m_2)l_1\int_0^t \ddot{x}_r^2 d\tau.\end{aligned} \tag{22}$$

Through the analysis of Principle 1, the following conclusions can be drawn as follows [38]:

$$x_r, \dot{x}_r, \ddot{x}_r, {x_r}^{(3)} \in L_\infty. \tag{23}$$

According to Principle 1, and then by using partial integration and scaling it, the result can be stated [38]

$$\begin{aligned}\int_0^t \ddot{x}_r^2 d\tau &\le \int_0^\infty \ddot{x}_r^2 d\tau \\ &\le \dot{x}_r \ddot{x}_r|_0^\infty - \int_0^\infty \dot{x}_r {x_r}^{(3)} d\tau \\ &< 2 v_{x\max} a_{x\max} + 2 j_{x\max} p_{dx} \\ &\Rightarrow \ddot{x}_r \in L_2 \cap L_\infty. \end{aligned} \tag{24}$$

In combination with (23)-(24), (22) is scaled and collated as follows:

$$\begin{aligned} V(t) &\le V(0) + \frac{1}{4}(m_1 + m_2) l_1 \\ &\quad \times (v_{x\max} a_{x\max} + j_{x\max} p_{dx}) \\ &\ll +\infty. \end{aligned} \tag{25}$$

Based on Principle 1 and (14), (22), (24)-(25), the results can be obtained

$$\begin{aligned} V(t) \in L_\infty &\Rightarrow e_\chi,\ \dot{e}_\chi,\ \dot{\theta}_1,\ \dot{\theta}_2 \in L_\infty \\ &\Rightarrow x,\ \dot{x},\ F_x,\ F_{rx} \in L_\infty. \end{aligned} \tag{26}$$

Equations (23)-(25) are combined, and the term of (22) is shifted, the following equation can be deduced

$$\begin{aligned} & k_{dx} \int_0^t \dot{e}_\chi^2 d\tau + d_{\theta_1} \int_0^t \dot{\theta}_1^2 d\tau + d_{\theta_2} \int_0^t \dot{\theta}_2^2 d\tau \\ & \le V(0) - V(t) + \frac{1}{4}(m_1 + m_2) \\ & \quad \times l_1 (v_{x\max} a_{x\max} + j_{x\max} p_{dx}) \\ & \ll +\infty \\ & \Rightarrow \dot{e}_\chi,\ \dot{\theta}_1,\ \dot{\theta}_2 \in L_2 \cap L_\infty. \end{aligned} \tag{27}$$

By substituting the relevant conclusions of (24)-(26) into the system dynamics model of double pendulum underactuated gantry crane, the following conclusions can be drawn

$$\ddot{x},\ \ddot{\theta}_1,\ \ddot{\theta}_2,\ \ddot{e}_\chi \in L_\infty. \tag{28}$$

The conclusions of (27)-(28) are combined, and the extended Barbalat theorem is used [40], and then the conclusions are as follows:

$$\lim_{t\to\infty} \left[\dot{e}_\chi(t) \quad \dot{\theta}_1(t) \quad \dot{\theta}_2(t)\right]^T = [0 \quad 0 \quad 0]^T. \tag{29}$$

By substituting (16) and (29) into (4)-(6), the following conclusions can be drawn at that time

$$\begin{cases} (M + m_1 + m_2)\ddot{e}_\chi + m_2 l_2 \ddot{\theta}_2 c_2 \\ \quad + (m_1 + m_2) l_1 \ddot{\theta}_1 c_1 = -k_{px} e_\chi, \\ m_2 l_2 \ddot{\theta}_2 c_{1-2} + (m_1 + m_2) \\ \quad \times \left[\ddot{e}_\chi c_1 + l_1 \ddot{\theta}_1 + g s_1\right] = 0, \\ \ddot{e}_\chi c_2 + l_1 \ddot{\theta}_1 c_{1-2} + l_2 \ddot{\theta}_2 + g s_2 = 0, \end{cases} \tag{30}$$

where $\lim_{t\to\infty} \ddot{e}_\chi = \lim_{t\to\infty} \ddot{x} - \ddot{x}_r - \lambda_1 l_1 \dot{\theta}_1 - \lambda_2 l_2 \dot{\theta}_2 = \ddot{x}$.

The first derivative of (30) is derived, and then the conclusions of (26) and (29) are substituted into the first derivative. It can be inferred that: $\lim_{t\to\infty} x^{(3)}$, $\lim_{t\to\infty} {\theta_1}^{(3)}$, $\lim_{t\to\infty} {\theta_2}^{(3)} \in L_\infty$.

The conclusions in (29) are combined, and then the extended Barbalat Theorem [40] is used. It can be seen that

$$\begin{aligned} &\lim_{t\to\infty} \ddot{e}_\chi(t) = \lim_{t\to\infty} \ddot{x}(t) = 0, \\ &\lim_{t\to\infty} \ddot{\theta}_1(t) = \lim_{t\to\infty} \ddot{\theta}_2(t) = 0. \end{aligned} \tag{31}$$

In connection with (30)-(31), the following results can be deduced:

$$\lim_{t\to\infty} \left[e_\chi(t) \quad \theta_1(t) \quad \theta_2(t)\right]^T = [0 \quad 0 \quad 0]^T. \tag{32}$$

$\dot{e}_\chi = \dot{x} - \lambda_1 l_1 \sin\theta_1 - \lambda_2 l_2 \sin\theta_2 - \dot{x}_r$ is known, and then the conclusions of (29), (32) and $\lim_{t\to\infty} \dot{x}_r(t) = 0$ are combined, the equation can be deduced

$$\lim_{t\to\infty} \dot{e}_\chi = \lim_{t\to\infty} \dot{x} = 0. \tag{33}$$

Equations (12) and (32) are combined simultaneously, and then, with the help of Principle 1, it can be inferred that

$$\lim_{t\to\infty} x(t) = p_{dx}. \tag{34}$$

When the conclusions of (29), (31)-(33) are combined, the conclusions can be obtained

$$\begin{aligned} &\lim_{t\to\infty} \left[x(t) \quad \dot{x}(t) \quad \theta_1(t) \quad \dot{\theta}_1(t) \quad \theta_2(t) \quad \dot{\theta}_2(t)\right]^T \\ &= [p_{dx} \quad 0 \quad 0 \quad 0 \quad 0 \quad 0]^T. \end{aligned}$$

According to the above equations, it can be known that the state variables of the double pendulum underactuated gantry crane system approaches to the equilibrium stable described in Theorem 1 gradually.

At this point, the proof is complete. □

4. NUMERICAL SIMULATION AND EXPERIMENTAL VERIFICATION

In MATLAB/SIMULINK, The double pendulum underactuated gantry crane system dynamic model is built, and a series of simulations are performed in this environment to prove the control effect of the proposed method. Firstly, the tracking method [23], saturation method [22] and time-varying sliding mode control method of variable parameter (VP-TVSMC method) [41] are compared with the proposed method to attest the excellent effect of the proposed method; and then, the crane experiment system is built. Combined with the simulation results, the actual feasibility is verified by hardware experiments. Finally, the robustness of the method against the uncertainties of

Table 2. Simulation test parameters of double pendulum underactuated gantry crane system.

Symbol	Implication	Unit
M	10	kg
m_1	0.5	kg
m_2	1	kg
g	9.8	m/s^2
p_{dx}	1.5	m
f_{r0x}	4.4	NA
ε_x	0.01	NA
k_{rx}	-0.5	NA
d_x	0.3	NA
d_{θ_1}	0.05	NA
d_{θ_2}	0.05	NA

the system parameters and external disturbances is tested under the condition that the gains remain constant. The system parameters are shown in Table 2. Without special instructions, the initial displacement $x(0)$, initial system swing angles $\theta_1(0)$, $\theta_2(0)$ are set to 0; the cable lengths are set as $l_1 = 0.8$ m and $l_2 = 0.3$ m respectively.

The control gains, which ensure that the proposed method can achieve excellent control effects in simulations and experiments, are selected through the following steps:

1) The control gain λ_1 in (10) shall ensure the validity of (21), that is, λ_1 shall meet the condition: $\lambda_1 l_1 > 1$. Moreover, the control gain λ_2 in (10) must satisfy the condition in (20): $\lambda_2 = \frac{m_2}{(m_1+m_2)}\lambda_1$.
2) To guarantee the system stability, the position gain k_{px} in (14) needs to ensure the positive definiteness of Lyapunov function, that is, k_{px} should be a positive value; the velocity gain k_{dx} in (17) needs to ensure that (22)-(25) hold, k_{dx} should also be a positive value.

4.1. Comparative simulation analysis

In MATLAB/SIMULINK, the proposed method, tracking method, saturation method and VP-TVSMC method are fully debugged, and a set of control gains with optimal control performance are selected respectively. Among them, the gains of the proposed method are $\lambda_1 = 3$, $k_{px} = 8$, $k_{dx} = 16$; the gains of tracking method are adjusted to $k_{px} = 1$, $k_{dx} = 80$; the gains of the saturation method are selected as $\alpha = -1$, $k_{px} = 6$, $k_{dx} = 17.5$; the gains of VP-TVSMC method are set as $K = 10$, $\varepsilon = 0.35$, $K_c = 2$, $K_\alpha = 2$, $\alpha = -26.3$, $\beta = 20$. Finally, the desired trajectory parameters are selected as $k_v = 0.9$, $k_a = 0.5$, $\varepsilon = 3.5$.

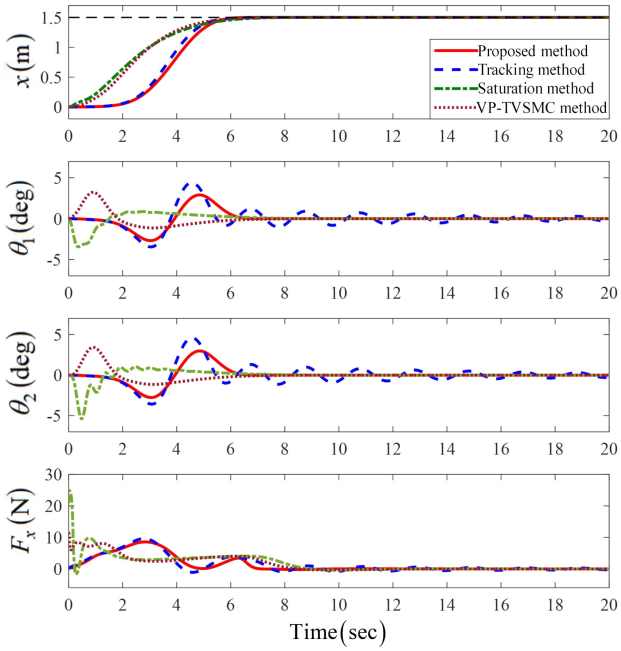

Fig. 3. Comparative simulation results of the four methods.

Then, the four methods are compared and verified, and the comparison results (see Fig. 3) and the quantitative performance index results (see Table 3) were obtained.

The indicators are described as follows:

1) $\theta_{i\max}$, $i = 1, 2$ stands for the maximum hook/load swing angle when the crane is in operation .
2) $\theta_{i\text{res}}$, $i = 1, 2$ stands for the maximum hook/load swing angle after the crane stops lifting.
3) t_{st} is the time taken for the crane to lift the load.

From the quantitative performance indicators in Table 3 and the comparative simulation results in Fig. 3, the positioning of the proposed method, tracking method, saturation method and VP-TVSMC method is all extremely accurate, and the final errors are controlled within 2 mm. Moreover, these four method spend a little time to complete the lifting load. The proposed method can ensure that the hook/load swing angle is controlled within 3 deg

Table 3. Quantitative performance index results.

Methods	p_{dx} (m)	$\theta_{1\max}$ (deg)	$\theta_{2\max}$(deg)	θ_{1res}(deg)	θ_{2res}(deg)	t_{st}(s)
Proposed method	1.5	2.88	2.97	0.34	0.33	6.1
Tracking method	1.502	4.4	4.6	1.2	1.33	6.1
Saturation method	1.5	3.43	5.44	0.09	0.09	7.2
VP-TVSMC method	1.5	3.21	3.44	0.12	0.12	6.5

during the lifting process, and on the premise of ensuring that the load move to the expected position promptly and precisely, the hook/load residual swing angle decays to 0 rapidly. Compared with the proposed method, the hook/load swing angle remains larger under the operation of the other three methods. It is worth pointing out that under the action of the saturation method, although the hook/load swing angle and driving force have different degrees of mutation when the trolley starts, the hook/load swing angle decays to 0 rapidly. And the proposed method and tracking method are guaranteeing the smooth start-up and stable operation of trolley, and the hook/load swing more smooth. After the tracking method makes the trolley reach the expected position, there are still large hook/load residual swing angle, and there is repeated load swing phenomenon after the trolley reaches the expected position, the proposed method can ensure that the residual swing angle is attenuated without repeated swing. In summary, combined with the comparative simulation results and quantitative performance indicators, the proposed method has excellent anti-swing characteristics, high security and efficient lifting.

4.2. Experimental analysis

The proposed method has achieved preeminent control effect in MATLAB/SIMULINK environment, and has been verified in simulation. However, its actual control performance has not been proved strongly in the real environment. Therefore, the crane experimental system is built, and the practical control effect is tested under the condition that the gains and crane system parameters remain constant. The experimental system is described in Fig. 4. As shown in Fig. 4, the crane experimental system mainly consists of a 1000 W AC servo motor with coaxial encoder (2000 PPR), a trolley, a PC with motion control aboard, a gantry with tracks, a hook and a load. The forward and back movement of the trolley is driven by the AC servo motor, and its horizontal displacement is obtained and converted by the coaxial encoder connected to the AC servo motor. The displacement signal is collected and processed by the motion control aboard (high-speed DSP as the motion control core) in the motor braking and encoder control system, and then uploaded to PC.

The swing angle signals of the hook and load are mainly collected by the high precision angle sensor (SINDT02) in Fig. 4. Since the two measuring devices are the same, only the process of measuring the swing angle of the hook is introduced here. The angle sensor (horizontal installation) transmits the collected and processed hook swing angle signal to the PC in the form of data, and the PC uses the MATLAB/SIMULINK module to achieve the real-time window target. The PC generates control input commands according to the proposed method, and the motion control aboard in the motor braking and encoder control system transmits the input commands to the AC servo motor, and

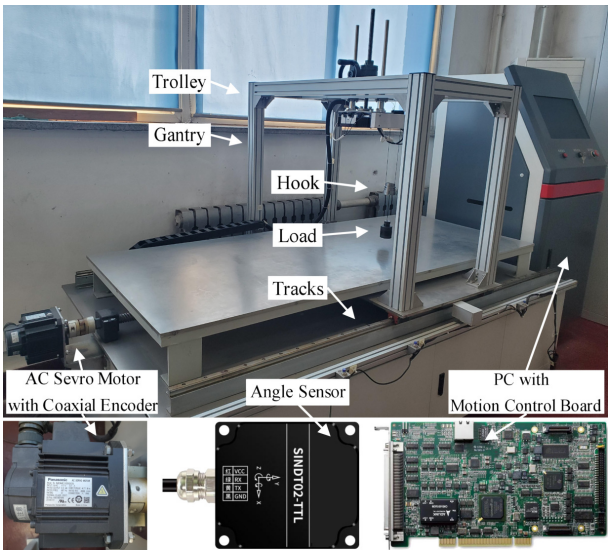

Fig. 4. Crane experimental system.

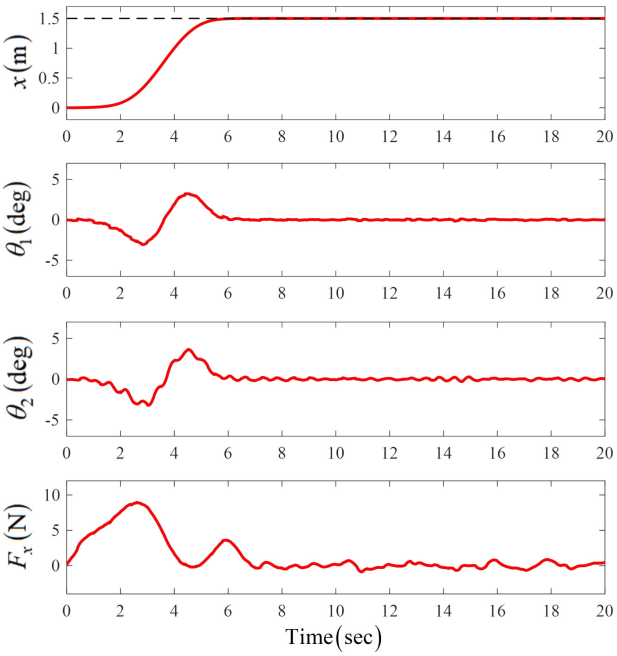

Fig. 5. Experiment results.

the control cycle is 10 ms.

Specifically, the designed control method is implemented by programming in C++ language on a PC. The trolley displacement signal, hook swing angle signal, load swing angle signal, driving force signal, etc. are transmitted to the PC in hexadecimal format and stored as txt files in real time. The program written in MATLAB software converts hexadecimal data into decimal data in real time, and displays them in graphical form through MATLAB/GUIDE and MATLAB/SIMULINK modules.

The experiment results are shown in Fig. 5. Through ex-

perimental measurement and data quantification, it can be seen that the actual final positioning errors of the trolley remain within ± 1 mm, and the actual transportation time of the trolley is similar to the simulation result. The actual maximum hook swing angle is 3.22 deg, and the actual maximum load swing angle is 3.63 deg. Compared with the simulation results, the actual system swing angles remain larger due to the existence of objective factors such as hardware accuracy and external interference, the swing curves of the hook and load have small fluctuations, but the overall curves tend to be smooth. In general, not only can the proposed method ensures the exact positioning of the trolley and effective anti-swing in the experiment, but also it ensures efficient lifting, and has certain practical application value.

4.3. Robustness verification

During the working process of gantry cranes, the working conditions are more complicated. Some system parameters (such as the load mass, expected displacement, cable length, and hook/load initial swing angle, etc.) are often difficult to measure accurately, and bridge cranes are inevitably affected. In addition, gantry cranes are inevitably affected by external factors (such as wind load and collision, etc.), which poses new challenges to the anti-swing effect of the proposed method. To test the robustness in response to these conditions, a series of comparative simulations are performed in MATLAB/SIMULINK under the condition that the control gains remain unchanged. The tests are divided into the following five situations:

Case 1: In the actual operation of gantry cranes, the mass of the load (such as the port container, etc.) varies greatly and is difficult to be measured accurately, which may affect the precise positioning of the trolley, lead to large system swing angles, and even affect the security of the operation. Therefore, it is of necessity to test the robustness against different load masses. For this purpose, the following three different load masses are used:

1) $m_2 = 1$ kg; 2) $m_2 = 0.2$ kg; 3) $m_2 = 5$ kg

The results of the first case are shown in Fig. 6. Under the condition of different load masses, the proposed method can still ensure that the load reaches the expected position accurately, and can suppress and eliminate system swing angle effectively. To be precise, the final positioning is 1.5 m, the transportation time is 6.1 s, and the hook/load swing angle is controlled within 3 deg. And under the operation of the proposed method, the changes of the load mass do not make the effect of the proposed method attenuated. Therefore, the proposed method has strong robustness when dealing with different load mass.

Case 2: When gantry cranes transports, the expected position of the trolley, which cannot be generalized, changes according to the difference of the expected position of the load. To test the robustness against different expected displacements, three different expected displacements are adopted as follows:

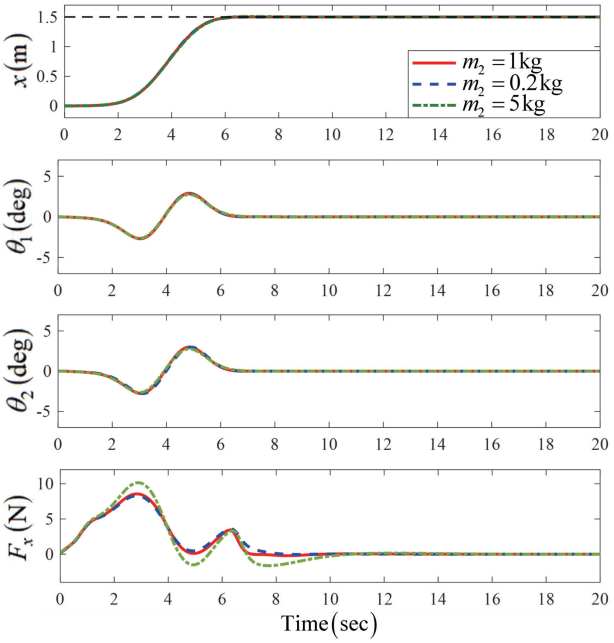

Fig. 6. Results of the first case.

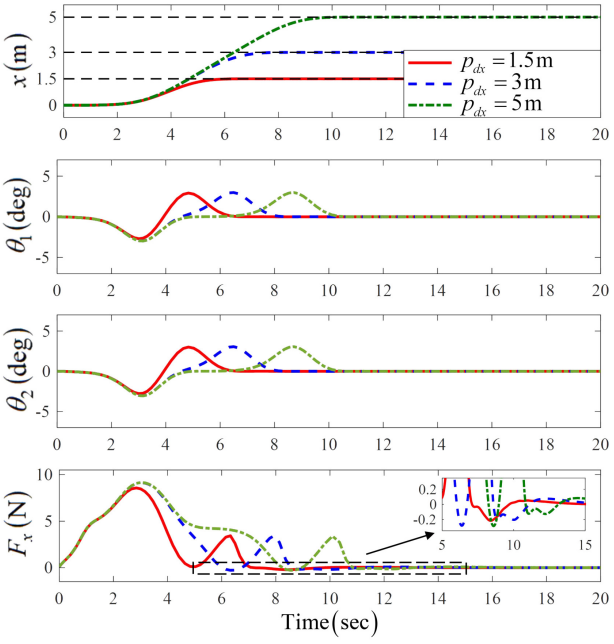

Fig. 7. Results of the second case.

1) $p_{dx} = 1.5$ m; 2) $p_{dx} = 3$ m; 3) $p_{dx} = 5$ m

The results of the second case are shown in Fig. 7. Under the action of the proposed method, the load is transported to different expected positions accurately, and the final positioning displacements are 1.5 m, 3 m and 5 m

respectively. Moreover, the lifting is fast and efficient, and the lifting time is 6.1 s, 7.7 s and 10 s respectively. During the whole lifting process, the maximum hook/load swing angle is controlled within 3 deg, and the residual hook/load swing angle decays to 0 rapidly after the trolley reaches the expected position. Therefore, the proposed method still has strong robustness when the expected displacements remain changed.

Remark 2: It is worth noting that in Fig. 7, driving force F_x is not always positive. Because its negative values are small, the negative values are not clearly shown in Fig. 7. In addition, in order to prevent frequent positive and negative changes of the motor, the negative values of driving force F_x are avoided as far as possible when adjusting the control gains.

Case 3: When establishing the gantry crane dynamic model and method design, to guarantee the system stability, it is of necessity to assume that the system swing angles remain 0. However, in most cases, it is inevitable that the system swing angles are not 0. Therefore, it is of necessity to test the robustness for various initial system swing angles. For this reason, the following three different sets of initial swing angles are used:

1) $\theta_1 = 0$ deg, $\theta_2 = 0$ deg;
2) $\theta_1 = 3$ deg, $\theta_2 = 5$ deg;
3) $\theta_1 = -3$ deg, $\theta_2 = -5$ deg

The results are shown in Fig. 8. When the system has different initial swing angles, the proposed method can still guarantee that the trolley reaches the expected position precisely, and the final positioning error can be controlled within ± 1 mm. And the lifting time has no obvious change. Under the action of the method, the hook/load swing angle is eliminated quickly. During the lifting process, the system swings remain smooth, and the residual swing angles are eliminated rapidly. The proposed method has excellent robustness when dealing with different initial swing angles.

Case 4: When gantry cranes work at high altitude, in order to avoid collision and ensure secure operation, the hook height often changes to different degrees, and the change of the cable length is prone to cause the large swing of the system greatly. To test the robustness for various cable lengths, these cable lengths are used as follows:

1) $l_1 = 0.8$ m; 2) $l_1 = 0.4$ m; 3) $l_1 = 1.6$ m

The results are shown in Fig. 9. Under the condition of changing the cable length, the proposed method can still ensure the trolley to reach the expected position precisely, and the difference in arrival time is negligible. The hook/load swing angle remains guaranteed within a secure range, and the swing curve is relatively smooth. The proposed method still has excellent robustness to different cable lengths.

Case 5: Gantry cranes are often operated in non-laboratory environments (such as port container lifting, etc.), and are inevitably affected by external disturbance such as wind load or load collision, which can easily cause violent system swings, and the swings are difficult to eliminate quickly. To test the robustness in dealing with external disturbances, a sinusoidal disturbance signal with amplitude of 5 deg is added to the load swing angle of

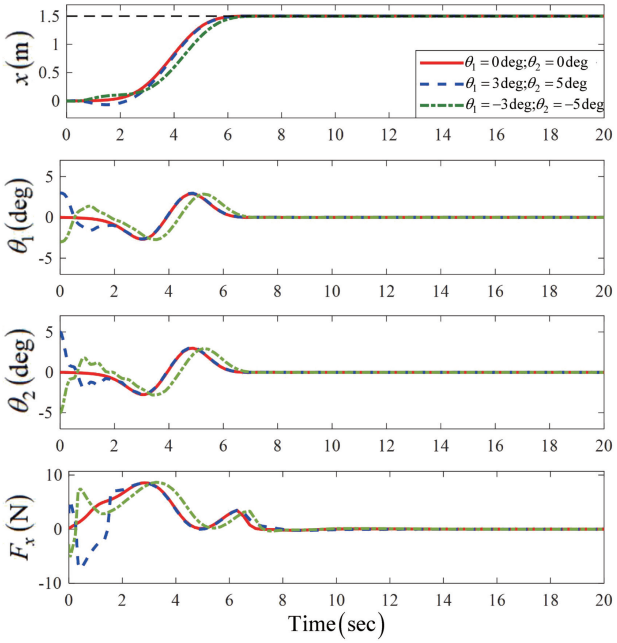

Fig. 8. Results of the third case.

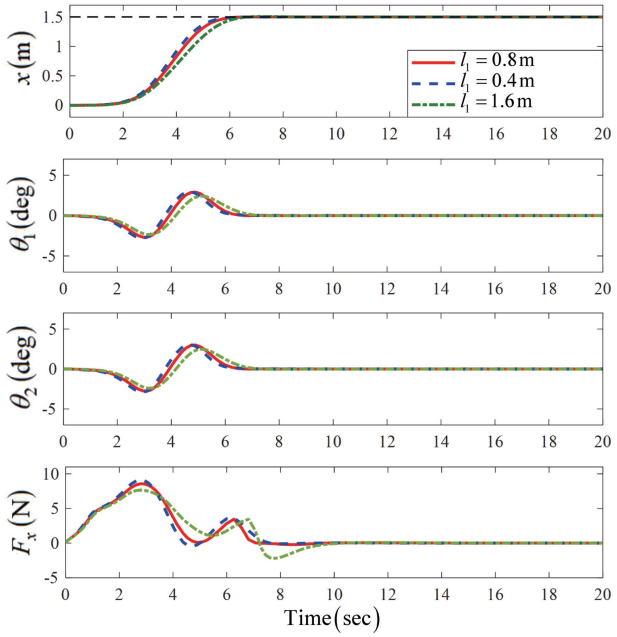

Fig. 9. Results of the fourth case.

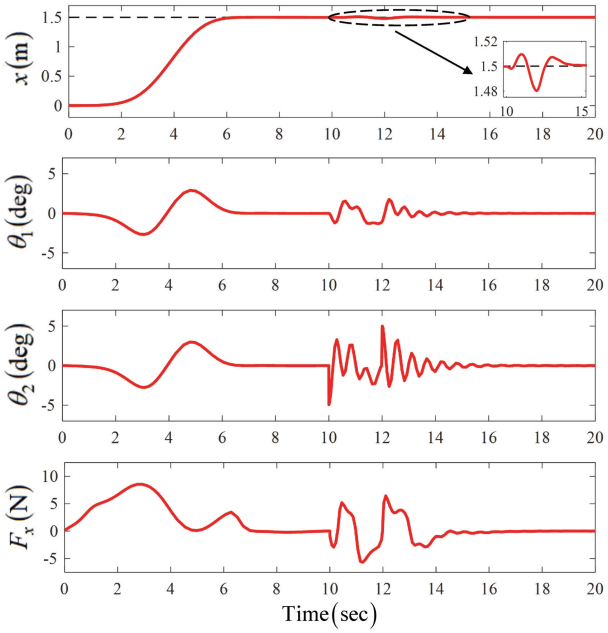

Fig. 10. Results of the fifth case.

the double pendulum underactuated gantry crane system at 10-12 s.

The results are shown in Fig. 10. When the double pendulum underactuated gantry crane system is disturbed by external disturbance, the proposed method can eliminate the external disturbance and restore the system to the equilibrium state without disturbance. To be precise, when the system is subjected to these disturbances, the position of the trolley does not fluctuate more than 20 mm, and the trolley can be restored to an accurate position after 5 s of the disturbance disappears. When the load is subjected to a sinusoidal disturbance with amplitude of 5 deg, the maximum hook swing angle is 1.76 deg, and the maximum load swing angle is 5 deg. The system swing angles are controlled within a secure range, and after 5 s of the external disturbance disappears, the system swing angles remain eliminated and restored to the original equilibrium state quickly. Therefore, when the system is given external disturbances, the proposed method has strong robustness to resist these external disturbances.

5. CONCLUSION

Aiming at the problems of low lifting efficiency, large hook/load swing angle, poor anti-interference ability and inaccurate positioning in the lifting process of double pendulum underactuated gantry cranes, an enhanced-coupling-based tracking control method is proposed. Compared with the tracking method, saturation method and VP-TVSMC method, the proposed method, which greatly improves the lifting efficiency of the gantry cranes, can restrain and eliminate the hook/load swing while ensuring the exact positioning of the trolley. To be precise, 1) under the action of the proposed method, which can save 15% of the lifting time, the final positioning error can be guaranteed within ± 1 mm, and the system swing angles are guaranteed within 3 deg; 2) the proposed method ensures the smooth start and stable operation of the trolley, and the system does not swing violently when the trolley starts/stops; 3) after crane stops lifting, the residual system swing angles is tiny and eliminated quickly; 4) the proposed method can still ensure the effective anti-swing and accurate positioning of the trolley with strong robustness under the condition of changing system parameters or adding external disturbances. In general, the proposed method, which has great practical significance and good application prospects, improves the working efficiency of the gantry cranes significantly, restrains and eliminates the system swings effectively, and provides a possibility for the research and development of the automatic driving of gantry cranes.

REFERENCES

[1] N. Sun, J. Y. Zhang, X. Xin, T. Yang, and Y. C. Fang, "Nonlinear output feedback control of flexible cable crane systems with state constraints," *IEEE Access*, vol. 7, pp. 136193-136202, September 2019.

[2] L. Ramli, Z. Mohamed, A. M. Abdullahi, H. I. Jaafar, and I. M. Lazim, "Control strategies for crane systems: A comprehensive review," *Mechanical systems and signal processing*, vol. 95, pp. 1-23, October 2017.

[3] H. T. Shi, G. Li, X. T. Bai, and J. Q. Huang, "Research on nonlinear control method of underactuated gantry crane based on machine vision positioning," *Symmetry*, vol. 11, no. 8, p. 987, August 2019.

[4] D. Chwa, "Sliding-mode-control-based robust finite-time antisway tracking control of 3-D overhead cranes," *IEEE Transactions on Industrial Electronics*, vol. 64, no. 8, pp. 6775-6784, August 2017.

[5] B. Lu, Y. C. Fang, and N. Sun, "Continuous sliding mode control strategy for a class of nonlinear underactuated systems," *IEEE Transactions on Automatic Control*, vol. 63, no. 10, pp. 3471-3478, October 2018.

[6] S. Frikha, M. Djemel, and N. Derbel, "A new adaptive neuro-sliding mode control for gantry crane," *International Journal of Control, Automation, and Systems*, vol. 16, no. 2, pp. 559-565, March 2018.

[7] X. Wu and X. He, "Nonlinear energy-based regulation control of three-dimensional overhead cranes," *IEEE Transactions on Automation Science and Engineering*, vol. 14, no. 2, pp. 1297-1308, April 2017.

[8] H. Wei and S. G. Shuzhi, "Cooperative control of a nonuniform gantry crane with constrained tension," *Automatica*, vol. 66, pp. 146-154, April 2016.

[9] N. Sun, Y. C. Fang, H. Chen, Y. M. Fu, and B. Lu, "Nonlinear stabilizing control for ship-mounted cranes with ship

roll and heave movements: Design, analysis, and experiments," *IEEE Transactions on Systems, Man, and Cybernetics: Systems*, vol. 48, no. 10, pp. 1781-1793, October 2018.

[10] F. Li, C. H. Zhang, and B. Sun, "A minimum-time motion online planning method for underactuated overhead crane systems," *IEEE Access*, vol. 7, pp. 54586-54594, April 2019.

[11] H. J. Peng, B. Y. Shi, X. W. Wang, and C. Li, "Interval estimation and optimization for motion trajectory of overhead crane under uncertainty," *Nonlinear Dynamics*, vol. 96, no. 6, pp. 1693-1715, April 2019.

[12] A. Elharfi, "Exponential stabilization and motion planning of an overhead crane system," *IMA Journal of Mathematical Control and Information*, vol. 34, no. 4, pp. 1299-1321, December 2017.

[13] H. Mohamed, S. Raafat, and S. Mostafa, "A hybrid partial feedback linearization and deadbeat control scheme for a nonlinear gantry crane," *Journal of the Franklin Institute*, vol. 355, no. 14, pp. 6286-6299, September 2018.

[14] B. Lu, Y. C. Fang, and N. Sun, "Enhanced-coupling adaptive control for double pendulum overhead cranes with payload hoisting and lowering," *Automatica*, vol. 101, pp. 241-251, March 2019.

[15] Z. Masoud, K. Alhazza, E. Abu-Nada, and M. Majeed, "A hybrid command-shaper for double pendulum overhead cranes," *Journal of Vibration and Control*, vol. 20, no. 1, pp. 24-37, January 2014.

[16] A. T. Le, G. H. Kim, and S. G. Lee, "Partial feedback linearization control of the three dimensional overhead crane," *IEEE International Conference on Automation Science and Engineering*, vol. 11, no. 4, pp. 718-727, March 2013.

[17] A. T. Le, S. G. Lee, and S. C. Moon, "Partial feedback linearization and sliding mode techniques for 2D crane control," *Transactions of the Institute of Measurement and Control*, vol. 36, no. 1, pp. 78-87, February 2014.

[18] M. H. Zhang and X. J. Jing, "Adaptive neural network tracking control for double-pendulum tower crane systems with nonideal inputs," *IEEE Transactions on Systems, Man, and Cybernetics: Systems*, vol. 52, no. 4, pp. 2514-2530, April 2022.

[19] N. Sun, Y. C. Fang, and H. Chen, "Adaptive antiswing control for cranes in the presence of rail length constraints and uncertainties," *Nonlinear Dynamics*, vol. 81, no. 1, pp. 41-51, July 2015.

[20] H. Chen, Y. C. Fang, and N. Sun, "A swing constraint guaranteed MPC algorithm for underactuated overhead cranes," *IEEE/ASME Transactions on Mechatronics*, vol. 21, no. 5, pp. 2543-2555, October 2016.

[21] Z. Wu, X. H. Xia, and B. Zhu, "Model predictive control for improving operational effificiency of overhead cranes," *Nonlinear Dynamics*, vol. 79, no. 4, pp. 2639-2657, March 2015.

[22] N. Sun, Y. C. Fang, H. Chen, and B. Lu, "Amplitude-saturated nonlinear output feedback antiswing control for underactuated cranes with double-pendulum cargo dynamics," *IEEE Transactions on Industrial Electronics*, vol. 64, no. 3, pp. 2135-2146, March 2017.

[23] M. H. Zhang, X. Ma, X. W. Rong, X. C. Tian, and Y. B. Li, "Adaptive tracking control for double pendulum overhead cranes subject to tracking error limitation, parametric uncertainties and external disturbances," *Mechanical Systems and Signal Processing*, vol. 76-77, pp. 15-32, August 2016.

[24] H. T. Shi, G. Li, X. Ma, and X. T. Bai, "Research on nonlinear coupling anti-swing control method of double pendulum gantry crane based on improved energy," *Symmetry*, vol. 11, no. 12, p. 1511, December 2019.

[25] M. H. Zhang and X. J. Jing, "A bioinspired dynamics-based adaptive fuzzy SMC method for half-car active suspension systems with input dead zones and saturations," *IEEE Transactions on Cybernetics*, vol. 51, no. 4, pp. 1743-1755, April 2021.

[26] M. H. Zhang, X. J. Jing, and G. Wang, "Bioinspired nonlinear dynamics-based adaptive neural network control for vehicle suspension systems with uncertain/unknown dynamics and input delay," *IEEE Transactions on Industrial Electronics*, vol. 68, no. 12, pp. 12646-12656, December 2021.

[27] M. H. Zhang, X. Ma, X. W. Rong, R. Song, X. C. Tian, and Y. B. Li, "Modeling and energy-based fuzzy controlling for underactuated overhead cranes with load transferring, lowering, and persistent external disturbances," *Advances in Mechanical Engineering*, vol. 9, no. 10, p. 168781401772008, October 2017.

[28] N. Sun, T. Yang, Y. C. Fang, Y. M. Wu, and H. Chen, "Transportation control of double-pendulum cranes with a nonlinear quasi-PID scheme: Design and experiments," *IEEE Transactions on Systems, Man, and Cybernetics: Systems*, vol. 49, no. 7, pp. 1408-1418, July 2019.

[29] H. Chen, B. K. Xuan, P. Yang, and H. Y. Chen, "A new overhead crane emergency braking method with theoretical analysis and experimental verification," *Nonlinear Dynamics*, vol. 98, no. 3, pp. 2211-2225, November 2019.

[30] M. H. Zhang, "Finite-time model-free trajectory tracking control for overhead cranes subject to model uncertainties, parameter variations and external disturbances," *Transactions of the Institute of Measurement and Control*, vol. 41, no. 10, pp. 1-10, February 2019.

[31] N. Sun, Y. M. Wu, Y. C. Fang, and H. Chen, "Nonlinear antiswing control for crane systems with double-pendulum swing effects and uncertain parameters: Design and experiments," *IEEE Transactions on Automation Science and Engineering*, vol. 15, no. 3, pp. 1413-1422, July 2018.

[32] M. H. Zhang, X. Ma, X. W. Rong, R. Song, X. C. Tian, and Y. B. Li, "A novel energy-coupling-based control method for double pendulum overhead cranes with initial control force constraint," *Advances in Mechanical Engineering*, vol. 10, no. 1, pp. 1-13, January 2018.

[33] N. Sun, Y. C. Fang, H. Chen, and B. He, "Adaptive nonlinear crane control with load hoisting/lowering and unknown parameters: Design and experiments," *IEEE/ASME Transactions on Mechatronics*, vol. 20, no. 5, pp. 2107-2119, October 2015.

[34] M. H. Zhang, Y. F. Zhang, and X. G. Cheng, "An enhanced coupling PD with sliding mode control method for underactuated double pendulum overhead crane systems," *International Journal of Control, Automation, and Systems*, vol. 17, no. 6, pp. 1579-1588, June 2019.

[35] X. Li, X. H. Peng, and Z. Y. Geng, "Anti-swing control for 2-D under-actuated cranes with load hoisting/lowering: A coupling-based approach," *ISA Transactions*, vol. 95, pp. 372-378, December 2019.

[36] A. T. Le, S. G. Lee, D. H. Ko, and L. C. Nho, "Combined control with sliding mode and partial feedback linearization for 3D overhead cranes," *International Journal of Robust and Nonlinear Control*, vol. 24, no. 18, pp. 3372-3386, December 2014.

[37] D. Chwa, "Sliding-mode-control-based robust finite-time antisway tracking control of 3-D overhead cranes," *IEEE Transactions on Industrial Electronics*, vol. 64, no. 8, pp. 6775-6784, August 2017.

[38] N. Sun and Y. C. Fang, "Nonlinear tracking control of underactuated cranes with load transferring and lowering: Theory and experimentation," *Automatica*, vol. 50, no. 9, pp. 2350-2357, September 2014.

[39] H. Chen and N. Sun, "Nonlinear control of underactuated systems subject to both actuated and unactuated state constraints with experimental verification," *IEEE Transactions on Industrial Electronics*, vol. 67, no. 9, pp. 7702-7714, September 2020.

[40] H. K. Khalil, *Nonlinear Systems*, 3rd Edition, Prentice Hall, Upper Saddle River, 2002.

[41] T. L. Wang, N. L. Nan, X. W. Zhang, G. Z. Li, S. Q. Su, J. Zhou, J. Z. Qiu, Z. Q. Wu, Y. K. Zhai, R. Labati, V. Piuri, and F. Scotti, "A time-varying sliding mode control method for distributed-mass double pendulum bridge crane with variable parameters," *IEEE Access*, vol. 9, pp. 75981-75992, May 2021.

Huaitao Shi received his B.S. and Ph.D. degrees in control engineering from Northeastern University, Shenyang, China, in 2005, and 2012, respectively. He has been a Professor with the Faculty of Mechanical Engineering, Shenyang Jianzhu University, Shenyang, where he has also been the Vice Dean, since 2014. He is the author of more than 40 articles, (26 articles were indexed by SCI), and six patents. His current research interests include research on nonlinear underactuated system and hybrid ceramic ball-bearing.

Fuxing Yao was born in Binzhou, Shandong, in 1996. He received his B.S. degree in mechanical design, manufacturing and automation from University of Jinan, Jinan, China, in 2019. He is currently pursuing a Master's degree in mechanical engineering with the School of Mechanical Engineering, Shenyang Jianzhu University, Shenyang, China. His research interest is automatic control of underactuated cranes.

Zhe Yuan received his Ph.D. degree in mechanical design from Northeastern University, Shenyang, China, in 2010. He has been a vice Professor with the Faculty of Mechanical Engineering, Shenyang Jianzhu University, Shenyang. His current research interests include research on nonlinear underactuated system and reliability of hybrid ceramic ball-bearing.

Yunjian Hu received his B.S. and Ph.D. degrees in control engineering from Northeastern University, Shenyang, China, in 2010, and 2020, respectively. He has been a lecturer with the Faculty of Mechanical Engineering, Shenyang Jianzhu University, Shenyang. His current research interests include cold-rolled strip rolling process control and the application of intelligent control in the rolling process, as well as the intelligent control of underactuated cranes.

Ke Zhang received his Ph.D. degree in mechanical manufacturing and automation from Northeastern University, Shenyang, China, in 2007. He has been a Professor with the Faculty of Mechanical Engineering, Shenyang Jianzhu University, Shenyang, where he has also been the Vice President, since 2018. He is the author of more than 210 articles. His main research interests include precision machining technology, construction equipment, and CNC equipment and technology.

Ling Fu is a researcher-level senior engineer. She is currently the chief engineer of Zoomlion, the dean of the Academia Sinica, and the director of the State Key Laboratory of Construction Machinery Key Technology. She is the author of more than 10 articles. Her research interests include mechanical equipment design and manufacturing technology research.